21. Watanabe T, Totoki Y, Toyoda A, Kaneda M, Kuramochi-Miyagawa S, Obata Y, *et al.* Endogenous siRNAs from naturally formed dsRNAs regulate transcripts in mouse oocytes. *Nature* 2008;**453:**539–543.
22. Lee Y, Kim M, Han J, Yeom KH, Lee S, Baek SH, *et al.* MicroRNA genes are transcribed by RNA polymerase II. *EMBO J* 2004;**23:**4051–4060.
23. Stanulovic VS, Kyrmizi I, Kruithof-de Julio M, Hoogenkamp M, Vermeulen JL, Ruijter JM, *et al.* Hepatic HNF4alpha deficiency induces periportal expression of glutamine synthetase and other pericentral enzymes. *Hepatology* 2007;**45:**433–444.
24. Yamada K, Watanabe M, Shibata T, Nagashima M, Tanaka K, Inoue Y. Glutamate transporter GLT-1 is transiently localized on growing axons of the mouse spinal cord before establishing astrocytic expression. *J Neurosci* 1998;**18:**5706–5713.
25. Buhler R, Lindros KO, Nordling A, Johansson I, Ingelman-Sundberg M. Zonation of cytochrome P450 isozyme expression and induction in rat liver. *Eur J Biochem* 1992;**204:**407–412.

## SUPPORTING INFORMATION ON THE INTERNET

The following supporting information may be found in the online version of this article.

**Table S1.** MicroRNA expression in $\beta$-catenin-deficient liver

Virchows Arch (2009) 454:513–517
DOI 10.1007/s00428-009-0762-6

ORIGINAL ARTICLE

# Esophageal melanomas harbor frequent *NRAS* mutations unlike melanomas of other mucosal sites

**Shigeki Sekine · Yukihiro Nakanishi · Reiko Ogawa · Satoko Kouda · Yae Kanai**

Received: 4 January 2009 / Revised: 26 February 2009 / Accepted: 8 March 2009 / Published online: 25 March 2009


**Abstract** Mucosal melanomas have genetic alterations distinct from those in cutaneous melanomas. For example, *NRAS*- and *BRAF*-activating mutations occur frequently in cutaneous melanomas, but not in mucosal melanomas. We examined 16 esophageal melanomas for genetic alterations in *NRAS*, *BRAF*, and *KIT* to determine whether they exhibit genetic features common to melanomas arising from other mucosal sites. A sequencing analysis identified *NRAS* mutations in six cases; notably, four of these mutations were located in exon 1, an uncommon mutation site in cutaneous and other mucosal melanomas. *BRAF* and *KIT* mutations were found in one case each. Immunohistochemistry showed KIT expression in four cases, including the tumor with a *KIT* mutation and two other intramucosal tumors. The low frequency of *BRAF* mutations and the presence of a *KIT* mutation-positive case are findings similar to those of mucosal melanomas of other sites, but the prevalence of *NRAS* mutations was even higher than that of cutaneous melanomas. The present study implies that esophageal melanomas have genetic alterations unique from those observed in other mucosal melanomas.

**Keywords** *NRAS* · *BRAF* · *KIT* · Esophageal melanoma

## Introduction

Melanomas show distinct patterns of genetic alterations depending on their sites of origin. The anatomical site-specific patterns of genetic alterations have been discussed in relation to the extent of ultraviolet exposure. *NRAS* and *BRAF* are the most frequently mutated oncogenes in melanomas. Both mutant N-Ras and B-Raf promote tumorigenesis through the constitutive activation of the MAP kinase pathway. Earlier studies suggested that *NRAS* mutations were frequent among melanomas arising from sun-exposed skin [1, 2]. Subsequently, *BRAF*-activating mutations were also identified in a significant proportion of melanomas [3]. Curtin et al. analyzed *NRAS* and *BRAF* mutations as well as DNA copy number changes in a large cohort of melanomas [4]. They utilized the presence of solar elastosis as a histological hallmark of chronic sun exposure and indicated that the majority of melanomas occurring on skin without chronic sun-induced damage had either *NRAS* or *BRAF* mutations whereas melanomas arising on skin with chronic sun-induced damage, acral sites, and mucosal membranes had mostly wild-type *NRAS* and *BRAF*. At the same time, they demonstrated that each group of melanomas exhibited distinct patterns of DNA copy number changes.

In addition to *NRAS* and *BRAF* mutations, a subset of melanomas contains *KIT* mutations [5–7]. Remarkably, the prevalence of *KIT* mutations also varies depending on the site of tumor origin, with the highest prevalence observed in mucosal melanomas [5]. Thus, genetic alterations in melanomas show site/organ-specific patterns and mucosal melanomas have distinct genetic features from those of cutaneous melanomas.

Esophageal melanomas are exceedingly rare, but highly aggressive neoplasms [8–10]. Previous studies have reported that melanomas constitute only 0.1–0.3% of all esophageal tumors [11, 12]. The rarity of this tumor is reasonable, considering the fact that the esophagus usually lacks melanocytes [13]. In addition, the esophagus is not

S. Sekine · Y. Nakanishi · R. Ogawa · S. Kouda · Y. Kanai (✉)
Pathology Division, National Cancer Center Research Institute,
5-1-1, Tsukiji, Chuo-ku,
Tokyo, Japan
e-mail: ykanai@ncc.go.jp

exposed to ultraviolet radiation, a major risk factor for melanomas. Because of the rarity of this lesion, data on genetic alterations in esophageal melanomas is scarce. However, the characterization of their genetic features, including how they differ from cutaneous melanomas and melanomas of other mucosal sites would contribute to the understanding of site/organ-specific genetic alterations in melanomas. Furthermore, considering the development of specific kinase inhibitors, such information could be critical for choosing an appropriate treatment. In this paper, we present the results of a mutational analysis of *NRAS*, *BRAF*, and *KIT* in 16 cases of esophageal melanomas.

## Materials and methods

Sixteen surgically resected esophageal melanomas were examined in the present study (Table 1). The samples were routinely fixed with 10% formalin and embedded in paraffin. Five-micrometer-thick sections of each specimen were stained briefly with hematoxylin and eosin and used for DNA extraction. The tumor and nontumor areas were separately dissected using sterilized toothpicks under a microscope. Tissues obtained from the proper muscle layer distant from the tumors were used as nontumor samples. The dissected samples were incubated in 100 μL of DNA extraction buffer (50 mmol/L Tris–HCl, pH 8.0, 1 mmol/L ethylenediaminetetraacetic acid, 0.5% (*v*/*v*) Tween 20, 200 μg/mL proteinase K) at 37°C overnight. Proteinase K was inactivated by heating at 100°C for 10 min. The DNA samples were subjected to polymerase chain reaction (PCR) directly or after purification. When required, the samples were purified using a QIAquick PCR Purification Kit (Qiagen, Hilden, Germany). PCR was performed for 3 min at 95°C for initial denaturing, followed by 35 or 40 cycles at 94°C for 15 s, 58°C for 20 s, and 72°C for 60 s and a final extension at 72°C for 5 min. The primers that were used are listed in Table 2. The PCR products were electrophoresed in a 2% (*w*/*v*) agarose gel, visualized under UV light with ethidium bromide staining, and recovered using a QIAquick Gel Extraction Kit (Qiagen). Isolated PCR products were sequenced bidirectionally on an Applied Biosystems 3130 Genetic Analyzer (Applied Biosystems, Foster, CA, USA) using the same primers used for amplification. Each experiment, including DNA extraction, was done at least twice.

Immunohistochemical staining was performed using the avidin–biotin complex method. The primary antibody used was polyclonal anti-KIT (A4502; 1:100 dilution; Dako, Denmark). 3-3′-Diaminobenzidine tetrahydrochloride was used as a chromogen. The sections were counterstained with hematoxylin. Mast cells in the sections were used as positive controls. For negative controls, the tissue was processed in the same way but the primary antibody was omitted. The staining

**Table 1** Results of mutational analysis and immunohistochemistry

| Case no. | Age/sex | Depth of invasion | *BRAF* | | *NRAS* | | *KIT* | | KIT IHC |
|---|---|---|---|---|---|---|---|---|---|
| | | | Nucleotide | Amino acid | Nucleotide | Amino acid | Nucleotide | Amino acid | |
| 1 | 62/M | Mucosa | – | | – | | – | | +++ (membranous) |
| 2 | 67/M | Mucosa | – | | – | | – | | +++ (membranous) |
| 3 | 48/M | Submucosa | – | | – | | – | | – |
| 4 | 57/F | Submucosa | – | | A183T | Q61H | – | | – |
| 5 | 64/M | Submucosa | – | | – | | – | | – |
| 6 | 67/M | Submucosa | – | | – | | – | | – |
| 7 | 72/M | Submucosa | – | | G35C | G12A | – | | – |
| 8 | 73/M | Submucosa | – | | – | | – | | – |
| 9 | 48/M | Muscularis propria | – | | – | | C1727T | L576P | +++ (cytoplasmic) |
| 10 | 68/M | Muscularis propria | T1799A | V600E | – | | – | | – |
| 11 | 69/M | Muscularis propria | – | | G34C | G12R | – | | – |
| 12 | 70/M | Muscularis propria | – | | G38C | G13A | – | | – |
| 13 | 63/M | Adventitia | – | | A183T | Q61H | – | | – |
| 14 | 64/M | Adventitia | – | | – | | – | | – |
| 15 | 68/M | Adventitia | – | | G37C | G13R | – | | – |
| 16 | 71/M | Adventitia | – | | – | | – | | ++ (membranous) |

*IHC* immunohistochemistry

**Table 2** Primers used in the present study

| | Forward primer | Reverse primer |
|---|---|---|
| *BRAF* exon15 | TGTTTGCTCTGATAGGAAAATG | CTGATGGGACCCACTCCAT |
| *NRAS* exon 1 | CAGGTTCTTGCTGGTGTGAAATGACTGAG | CTACCACTGGGCCTCACCTCTATGG |
| *NRAS* exon 2 | AACAAGTGGTTATAGATGGTGA | CGTTAGAGGTTAATATCCGCA |
| *KIT* exon 11 | TTTCCCTTTCTCCCCACAG | AAAGCCCCTGTTTCATACTGAC |
| *KIT* exon 13 | TGCTAAAATGCATGTTTCCAAT | CAGCTTGGACACGGCTTTAC |
| *KIT* exon 17 | TTTCTTTTCTCCTCCAACCTAA | TGTCAAGCAGAGAATGGGTACT |

results were evaluated based on the amount of immunopositive tumor cells as follows: − [<5%], + [5–25%], ++ [25–75%], +++ [>75%]. When KIT is expressed, the staining intensity and the subcellular localization were also evaluated.

## Results

The results of the mutational analysis are summarized in Table 1. A *BRAF* mutation was found in one case, while *NRAS* mutations were observed in six cases (Fig. 1). Four of six *NRAS* mutations were located in exon 1, and all these mutations were G to C transversions. All *BRAF* and *NRAS* mutations were missense mutations that had been previously identified as being oncogenic. A missense *KIT* mutation was observed in one case. The mutation affected the juxtamembrane domain of KIT. The wild-type sequence signal was very low for this mutation, suggesting that it was a homozygous mutation. All samples from nontumor areas showed wild-type sequences, indicating the somatic nature of the mutations. All the mutations that were observed were mutually exclusive.

Immunohistochemistry showed no or only focal and equivocal KIT expression in 12 cases (Fig. 2a). The case with the *KIT* mutation showed strong cytoplasmic expression (Fig. 2b), and another case showed heterogeneous staining with approximately 70% of the area exhibiting moderate membranous expression (Fig. 2c). Based on the heterogeneous KIT expression, we performed an additional mutational analysis. The KIT-positive and KIT-negative areas were separately subjected to sequencing analysis, but no *KIT* mutations were observed in either sample. Two early-stage melanomas limited to the mucosal layer exhibited strong and diffuse membranous KIT expression (Fig. 2d).

## Discussion

*NRAS* and *BRAF* mutations are the most common genetic alterations in melanomas. An extensive literature review by Hocker and Tsao reported overall mutation rates of 26% for *NRAS* and 42% for *BRAF* in cutaneous melanomas [14]. In contrast, several studies concurred that these mutations are significantly less prevalent in mucosal melanomas with reported frequencies of 5–14% for *NRAS* and 0–10% for *BRAF* [2, 4, 15–17].

Our results showed that *BRAF* mutations are uncommon among esophageal melanomas as in mucosal melanomas of other organs. Unexpectedly, however, six of the 16 melanomas were found to harbor *NRAS*-activating mutations. While our series may not be sufficiently large to determine the mutational frequency conclusively, the prevalence of *NRAS* mutation-positive cases in the present series was even higher than that observed in cutaneous melanomas. Notably, four of the six mutations were located in exon 1 of *NRAS* and all these mutations were G to C transversions. This finding is intriguing as *NRAS* mutations in melanomas predominantly affect codon 61 within exon 2 and G to C transversion is a rare type of mutations for these sites [14].

Furthermore, previous studies showed that a few recurrent mutations are responsible for the vast majority of *NRAS* mutations in melanomas. The literature review by Hocker and Tsao showed that three mutations, G35A, C181A, and A182G, accounted for 82% of *NRAS* mutations of the 255 substitutions at the *NRAS* locus [14]. However, surprisingly, none of the six mutations identified in this study were identical to these most common *NRAS* mutations. These observations suggest that esophageal melanomas have a high frequency of *NRAS* mutations with a unique mutation spectrum.

Our literature review identified only one study analyzing *NRAS* and *BRAF* mutations in esophageal melanomas. Wong et al. examined three cases of esophageal melanomas, two of which had *NRAS*-activating mutations affecting codons 12 and 61, respectively [17]. On the other hand, only two *BRAF* and three *NRAS* mutations were identified in 33 mucosal melanomas arising outside of the esophagus in their series. While the number of subjects in their study was small, their result is consistent with our finding that esophageal melanomas have a high prevalence of *NRAS* mutations.

A *KIT* mutation was identified in one case, indicating that a subset of esophageal melanomas harbor *KIT*-activating mutations as in other mucosal melanomas. An identical mutation has been reported in gastrointestinal

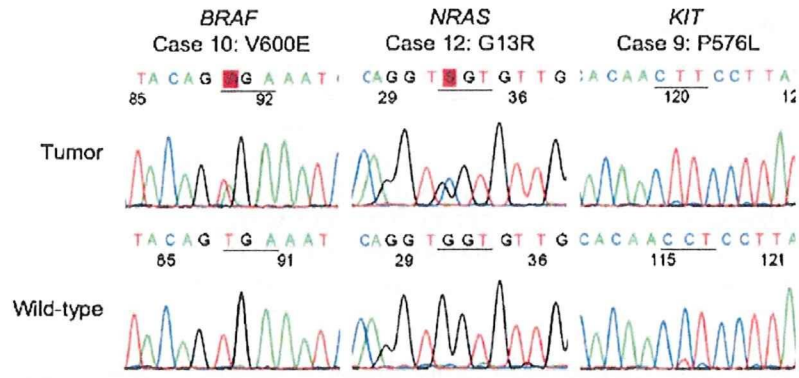


**Fig. 1** Representative mutations of *BRAF*, *NRAS*, and *KIT* in esophageal melanomas. Heterozygous *BRAF* V600E and *NRAS* G13R mutations and homozygous P576L *KIT* mutation are shown

stromal tumors and anal melanomas [7, 18], and this mutation has been shown to be associated with a sensitivity to dasatinib and imatinib, inhibitors of SRC/ABL and KIT [7]. While the frequency of this mutation was not high in the present series, the identification of a *KIT* mutation is important, since it provides an immediate therapeutic application. Indeed, the successful treatments of melanomas with *KIT* mutations by imatinib have been recently reported [19, 20].

Of note, the case with the *KIT* mutation also exhibited the strong expression of KIT protein, whereas the majority of the mutation-negative melanomas did not express KIT, as determined using immunohistochemistry. This finding agrees with the results of previous studies on mucosal melanomas of other sites and suggests that immunohistochemistry is useful for excluding *KIT* mutation-negative cases prior to genetic testing [6, 7]. We also found KIT expression in two early-stage tumors. The expression of KIT in early-stage cutaneous melanomas has also been previously reported [21, 22]. Since non-neoplastic melanocytes express KIT, the expression of KIT in early-stage melanomas might be regarded as the retention of physiological expression in melanocytes [21]. Overall, our observations suggest that immunohistochemistry for KIT may be useful for prescreening *KIT* mutation-positive cases among advanced esophageal melanomas.

The present study indicates that esophageal melanomas have a high frequency of *NRAS* mutations unlike mucosal melanomas of other sites. Furthermore, the mutational spectrum of *NRAS* is distinct from those commonly observed in melanomas. Even among mucosal melanomas, the patterns of genetic alterations are likely distinct between

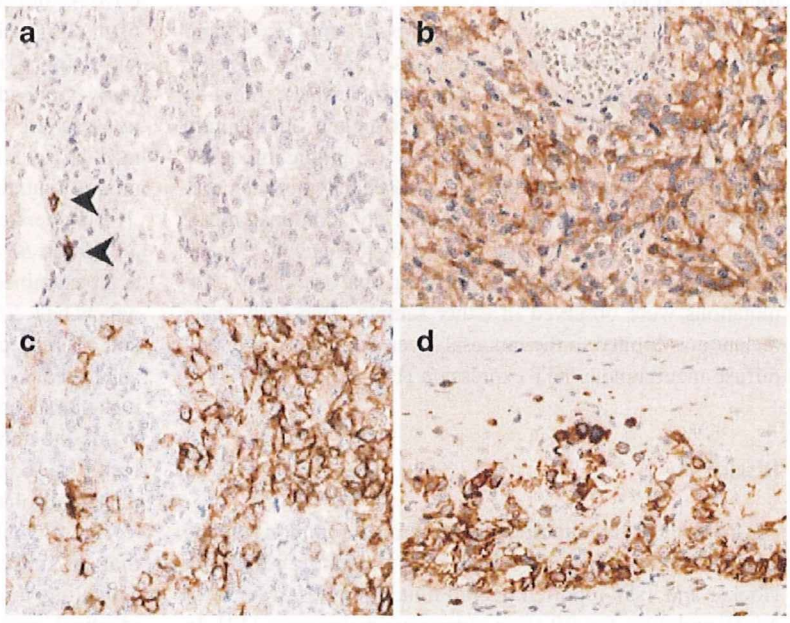


**Fig. 2** KIT expression in esophageal melanomas. **a** This case lacks KIT expression. Few mast cells show positive staining (*arrowheads*; case 13). **b** Tumor cells show diffuse cytoplasmic staining (case 9). **c** An area of the tumor cells shows membranous expression (case 16). **d** Tumor cells proliferating within the epithelial layer show membranous expression (case 2)

differing sites of origin. Our observations also suggest that not only the degree of ultraviolet exposure, but also organ-specific factors may significantly influence the mutational spectrum in melanomas.

**Acknowledgements** This work was supported by a Grant-in-Aid for the Third Term Comprehensive 10-Year Strategy for Cancer Control, a Grant-in-Aid for Cancer Research from the Ministry of Health, Labor and Welfare of Japan, and a program for promotion of Fundamental Studies in Health Sciences of the National Institute of Biomedical Innovation (NiBio), Japan.

**Conflicts of interest** The authors declare that they have no conflicts of interest.

## References

1. van't Veer LJ, Burgering BM, Versteeg R et al (1989) N-ras mutations in human cutaneous melanoma from sun-exposed body sites. Mol Cell Biol 9:3114–3116
2. Jiveskog S, Ragnarsson-Olding B, Platz A et al (1998) N-ras mutations are common in melanomas from sun-exposed skin of humans but rare in mucosal membranes or unexposed skin. J Invest Dermatol 111:757–761
3. Davies H, Bignell GR, Cox C et al (2002) Mutations of the BRAF gene in human cancer. Nature 417:949–954
4. Curtin JA, Fridlyand J, Kageshita T et al (2005) Distinct sets of genetic alterations in melanoma. N Engl J Med 353:2135–2147
5. Curtin JA, Busam K, Pinkel D et al (2006) Somatic activation of KIT in distinct subtypes of melanoma. J Clin Oncol 24:4340–4346
6. Rivera RS, Nagatsuka H, Gunduz M et al (2008) C-*kit* protein expression correlated with activating mutations in KIT gene in oral mucosal melanoma. Virchows Arch 452:27–32
7. Antonescu CR, Busam KJ, Francone TD et al (2007) L576P KIT mutation in anal melanomas correlates with KIT protein expression and is sensitive to specific kinase inhibition. Int J Cancer 121:257–264
8. Kato H, Watanabe H, Tachimori Y et al (1991) Primary malignant melanoma of the esophagus: report of four cases. Jpn J Clin Oncol 21:306–313
9. Li B, Lei W, Shao K et al (2007) Characteristics and prognosis of primary malignant melanoma of the esophagus. Melanoma Res 17:239–242
10. Lohmann CM, Hwu WJ, Iversen K et al (2003) Primary malignant melanoma of the oesophagus: a clinical and pathological study with emphasis on the immunophenotype of the tumours for melanocyte differentiation markers and cancer/testis antigens. Melanoma Res 13:595–601
11. Turnbull AD, Rosen P, Goodner JT et al (1973) Primary malignant tumors of the esophagus other than typical epidermoid carcinoma. Ann Thorac Surg 15:463–473
12. Scotto J, Fraumeni JF Jr, Lee JA (1976) Melanomas of the eye and other noncutaneous sites: epidemiologic aspects. J Natl Cancer Inst 56:489–491
13. Tateishi R, Taniguchi H, Wada A et al (1974) Argyrophil cells and melanocytes in esophageal mucosa. Arch Pathol 98:87–89
14. Hocker T, Tsao H (2007) Ultraviolet radiation and melanoma: a systematic review and analysis of reported sequence variants. Hum Mutat 28:578–588
15. Cohen Y, Rosenbaum E, Begum S et al (2004) Exon 15 BRAF mutations are uncommon in melanomas arising in nonsun-exposed sites. Clin Cancer Res 10:3444–3447
16. Edwards RH, Ward MR, Wu H et al (2004) Absence of BRAF mutations in UV-protected mucosal melanomas. J Med Genet 41:270–272
17. Wong CW, Fan YS, Chan TL et al (2005) BRAF and NRAS mutations are uncommon in melanomas arising in diverse internal organs. J Clin Pathol 58:640–644
18. Lasota J, Jasinski M, Sarlomo-Rikala M et al (1999) Mutations in exon 11 of c-*Kit* occur preferentially in malignant versus benign gastrointestinal stromal tumors and do not occur in leiomyomas or leiomyosarcomas. Am J Pathol 154:53–60
19. Hodi FS, Friedlander P, Corless CL et al (2008) Major response to imatinib mesylate in KIT-mutated melanoma. J Clin Oncol 26:2046–2051
20. Lutzky J, Bauer J, Bastian BC (2008) Dose-dependent, complete response to imatinib of a metastatic mucosal melanoma with a K642E KIT mutation. Pigment Cell Melanoma Res 21:492–493
21. Montone KT, van Belle P, Elenitsas R et al (1997) Proto-oncogene c-*kit* expression in malignant melanoma: protein loss with tumor progression. Mod Pathol 10:939–944
22. Janku F, Novotny J, Julis I et al (2005) KIT receptor is expressed in more than 50% of early-stage malignant melanoma: a retrospective study of 261 patients. Melanoma Res 15:251–256

CME/SAM

# Prognostic Significance of CXCL12 Expression in Patients With Colorectal Carcinoma

*Yuri Akishima-Fukasawa, MD, PhD,[1] Yukihiro Nakanishi, MD, PhD,[1] Yoshinori Ino,[1] Yoshihiro Moriya, MD, PhD,[2] Yae Kanai, MD, PhD,[1] and Setsuo Hirohashi, MD, PhD[1]*

**Key Words:** CXCL12; Invasive front; Immunohistochemistry; Colorectal carcinoma; Prognosis

DOI: 10.1309/AJCPK35VZJEWCUTL

Upon completion of this activity you will be able to:
- define the World Health Organization criteria for the histologic grading of the differentiation of colorectal carcinoma.
- discuss the role of examination of the invasive front of colorectal carcinoma for tumor budding and how this may pertain to prognosis.
- discuss the potential application of immunohistochemical staining for CXCL12 to highlight tumor budding in colorectal carcinoma.

The ASCP is accredited by the Accreditation Council for Continuing Medical Education to provide continuing medical education for physicians. The ASCP designates this educational activity for a maximum of 1 *AMA PRA Category 1 Credit* ™ per article. This activity qualifies as an American Board of Pathology Maintenance of Certification Part II Self-Assessment Module.

The authors of this article and the planning committee members and staff have no relevant financial relationships with commercial interests to disclose.

Questions appear on p 307. Exam is located at www.ascp.org/ajcpcme.

## Abstract

*The present study investigated the protein expression level of CXCL12 in colorectal cancer and aimed to elucidate its association with prognosis. CXCL12 positivity in 50% or more of tumor cells was defined as high expression and that in less than 50% of the tumor cells as low expression. CXCL12+ tumor budding at the invasive front was divided into 2 grades: high with 10 or more budding foci per ×200 field of view and low grade with fewer than 10 budding foci. Patients with high expression (72.7%) and high grade CXCL12+ tumor budding (43.0%) had significantly shorter survival than patients with low expression (*P = .014*) and low grade (*P = .003*), respectively. Patients with a combination of high expression and high grade had the worst outcome (*P < .001*). Our study demonstrated that CXCL12 expression in colorectal cancer cells and at sites of budding were significant prognostic factors. Furthermore, together with lymph node metastasis, a combination of both expression patterns was a more powerful independent prognostic factor.*

Several studies have revealed that the establishment of metastasis is the final outcome of a series of phenomena including tumor cell deposition in distant organs, clonogenic growth, and angiogenesis. These processes are fundamental for tumor cell survival and tumor metastasis and are regulated by interactions of cancer cells with the host microenvironment.[1-3] The CXC chemokine ligand-12 (CXCL12), stromal cell derived factor-1, is a member of the CXC chemokine family, which has been initially cloned from murine bone marrow and characterized as a pre B-cell growth-stimulating factor.[4-6] CXCL12 exerts effects through its physiologic cognate receptor, CXC chemokine receptor 4 (CXCR4), and is known to have roles in chemotaxis,[7] hematopoiesis,[8] and angiogenesis.[9,10] In addition, CXCR4 is involved in tumor cell homing to specific organs and in tumor progression.[11-13] CXCL12/CXCR4 also has a critical role in determining the metastatic destination of breast cancer cells.[12] It is also evident that some CXCR4+ tumors, including colorectal cancer,[1,13,14] exhibit marked malignant behavior.[12,15,16] So far, few studies have focused on chemokine expression in cancer cells,[17-21] and little is known about the clinicopathologic significance of CXCL12 expression in patients with colorectal cancer.

In this study, we attempted to evaluate the clinicopathologic significance of CXCL12 expression in patients with colorectal cancer by using immunohistochemical analysis together with examination of conventional histopathologic features.

## Materials and Methods

Between 1996 and 1997 at the National Cancer Center Hospital, Tokyo, Japan, 165 patients underwent surgery for primary colorectal carcinoma, including 100 colon (60.6%)

and 65 rectal (39.4%) cancers. Sample selection was restricted to consecutive cases diagnosed as stages II and III according to the International Union Against Cancer TNM classification.[22] Of the 165 cases, 72 (43.6%) were classified as stage II and 93 (56.4%) as stage III; 116 cases (70.3%) were T2-3, and 49 were T4 (29.7%).

All patients underwent curative resection, defined as the removal of gross cancer and the demonstration of tumor-negative surgical margins by histopathologic examination of the total circumference. No patients received preoperative chemotherapy, and all patients were free of distant visceral metastases. The patients comprised 101 men and 64 women, ranging in age from 32 to 93 years (mean – SD, 61.8 – 11.2 years). Postsurgical follow-up studies were completed for all patients, with follow-up periods ranging from 3 to 2,544 days (median, 1,844 days). Postsurgical recurrence was diagnosed by ultrasonography and computed tomography. This study was approved by the National Cancer Center Ethics Committee, Tokyo, Japan.

All available routinely processed, formalin-fixed, and paraffin-embedded blocks of colorectal carcinoma were obtained. Sections containing the maximum diameter of the tumor were used in the present study. Age, sex, tumor location, tumor size, macroscopic type, depth of tumor invasion, tumor differentiation, tumor budding grade by H&E staining, lymphatic vessel invasion, blood vessel invasion, lymph node metastasis, liver metastasis, and lung metastasis were subjected to statistical analyses **Table 1**.

The grade of tumor differentiation was decided on the basis of the predominant component in the tumor according to the World Health Organization classification: the percentage of the tumor showing formation of gland-like structures can be used to define the grade; well differentiated (grade 1) lesions exhibit glandular structures in more than 95% of the tumor; moderately differentiated (grade 2) adenocarcinoma has 50% to 90% glands; poorly differentiated (grade 3) adenocarcinoma has 5% to 50%; and undifferentiated (grade 4) carcinoma has less than 5%. Mucinous adenocarcinoma and signet-ring cell carcinoma, by convention, are considered poorly differentiated (grade 3).[23]

The existence of tumor budding at the invasive front was also evaluated. The invasive front in this study was defined as all regions of the border area between the primary tumor and interstitium in the submucosa, muscularis propria, subserosa, or nonperitonealized pericolonic/perirectal tissues. In accordance with previous studies, an isolated single cancer cell or a cluster composed of fewer than 5 cancer cells observed in the stroma of the actively invasive region was defined as a budding focus.[24-26] After reviewing the H&E-stained slides from each case, a field where the budding foci were most intense was selected. The number of budding foci was counted using a 20× microscope objective, giving a final magnification of ×200. A count ranging from 0 to 9 budding foci per field was designated as low grade and a count of 10 or more as high grade, in accordance with previous studies.[25,26]

### Immunohistochemical Studies

After deparaffinization, all sections were pretreated in citrate buffer (10 mmol/L, pH 6.0) at 121 C for 10 minutes for antigen retrieval. Endogenous peroxidase was blocked with 0.3% hydrogen peroxide in methanol for 20 minutes. The sections were then incubated with anti-CXCL12/SDF-1 monoclonal antibody (0.5 ng/mL; R&D Systems, Minneapolis, MN) at 4 C overnight. The immunostained sections were washed with phosphate-buffered saline and processed with an EnVision+ kit (DakoCytomation, Carpinteria, CA) in accordance with the manufacturer s instructions. Immunoproducts were visualized by using diaminobenzidine tetrahydrochloride, and the sections were counterstained with hematoxylin. As an internal positive control for CXCL12 staining, the immunopositivity of normal colorectal epithelia adjacent to the tumors and endothelial cells of blood vessels was used. Intensity of positive staining in tumor cells that was the same as or more than that in normal colorectal epithelia was considered positive. Sections from each paraffin block were used as negative control samples by replacing the primary antibody with normal mouse immunoglobulin. After immunohistochemical analysis, the tumors were categorized according to the ratio and localization of immunopositive tumor cells in the sections containing the maximum tumor diameter.

We examined the relationship between the CXCL12 positivity rate in tumor cells and various clinicopathologic factors and found that a cutoff value of 50% was the most powerful discriminatory factor. Accordingly, a cutoff index of 50% was selected for our study. When the proportion of tumor cells positive for CXCL12 was 50% or more, the tumor was defined as showing high CXCL12 expression, whereas tumors in which fewer than 50% of the cells were positive were defined as showing low CXCL12 expression.

In addition, CXCL12 expression in foci of tumor budding at the invasive front was quantified and scored by the same method as for evaluation of tumor budding grade using H&E-stained sections. After scanning each CXCL12-immunostained slide, a field where immunopositivity in the budding foci was the most intense was selected, and the number of CXCL12+ budding foci was counted at ×200 magnification. For all histopathologic variables, each macroscopic record and microscopic slide was analyzed by 2 experienced pathologists (Y.A.-F. and Y.N.) to reach a consensus.

### Statistical Analysis

The relationships between clinicopathologic characteristics and the number of immunopositive tumor cells were analyzed by variance tests when appropriate. The $\chi^2$ test was




DOI: 10.1309/AJCPK35VZJEWCUTL

used to analyze variables such as sex, tumor location, depth of tumor invasion, tumor differentiation, tumor budding grade assessed by H&E staining, lymphatic vessel invasion, blood vessel invasion, lymph node metastasis, liver metastasis, and lung metastasis. The Student *t* test was used for statistical comparisons of variables such as age and tumor size, and the Mann-Whitney *U* test was applied to compare the variables of macroscopic type. Survival was measured from the date of surgery to the end of the follow-up period or death. Overall survival curves were determined by using the Kaplan-Meier method and were analyzed by using the log-rank test. Univariate and multivariate survival analysis was performed by using the Cox proportional hazards regression model with the StatView, version 5.0 software package (SAS Institute, Cary, NC), in a stepwise manner.

## Results

### Expression of CXCL12 in Colorectal Cancer

Immunoreactivity of CXCL12 was observed in the cell membrane and/or cytoplasm of tumor cells **Image 1A**. The endothelial cells of blood vessels and normal intestinal epithelia, especially in the middle to upper third portion of the crypt,

**Table 1**
**Correlation of CXCL12 Expression With Clinicopathologic Features***

| | CXCL12 Expression | | | CXCL12+ Tumor Budding Grade | | | CXCL12 Expression and Tumor Budding Grade | | |
|---|---|---|---|---|---|---|---|---|---|
| Variable | Low (n = 45) | High (n = 120) | *P* | Low (n = 94) | High (n = 71) | *P* | Others (n = 99) | High Expression With High Grade (n = 66) | *P* |
| Age (y) | 62.9 ± 12.7 | 61.4 ± 10.7 | .319 | 61.9 ± 11.5 | 61.6 ± 11.0 | .778 | 62.4 ± 11.5 | 60.9 ± 10.8 | .346 |
| Sex | | | .986 | | | .192 | | | .096 |
| Male | 27 | 74 | | 53 | 48 | | 55 | 46 | |
| Female | 18 | 46 | | 41 | 23 | | 44 | 20 | |
| Tumor location | | | .525 | | | .622 | | | .625 |
| Colon | 25 | 75 | | 59 | 41 | | 62 | 38 | |
| Rectum | 20 | 45 | | 35 | 30 | | 37 | 28 | |
| Maximum tumor diameter (cm) | 4.7 ± 2.1 | 5.1 ± 1.9 | .155 | 5.1 ± 2.1 | 4.7 ± 1.6 | .232 | 5.0 ± 2.1 | 4.8 ± 1.6 | .589 |
| Macroscopic type† | | | .943 | | | .256 | | | .287 |
| 1 | 3 | 9 | | 10 | 2 | | 10 | 2 | |
| 2 | 42 | 109 | | 84 | 67 | | 89 | 62 | |
| 3 | 0 | 2 | | 0 | 2 | | 0 | 2 | |
| 4 | 0 | 0 | | 0 | 0 | | 0 | 0 | |
| Tumor depth‡ | | | .001 | | | <.001 | | | <.001 |
| T2, T3 | 40 | 76 | | 78 | 38 | | 81 | 35 | |
| T4 | 5 | 44 | | 16 | 33 | | 18 | 31 | |
| Tumor differentiation§ | | | >.999 | | | >.999 | | | >.999 |
| Grade 1/2 | 44 | 116 | | 91 | 69 | | 96 | 64 | |
| Grade 3/4 | 1 | 4 | | 3 | 2 | | 3 | 2 | |
| Tumor budding grade (H&E staining) | | | .013 | | | <.001 | | | <.001 |
| Low | 36 | 69 | | 78 | 27 | | 80 | 25 | |
| High | 9 | 51 | | 16 | 44 | | 19 | 41 | |
| Lymphatic vessel invasion | | | .984 | | | .324 | | | .559 |
| Present | 36 | 94 | | 71 | 59 | | 76 | 54 | |
| Absent | 9 | 26 | | 23 | 12 | | 23 | 12 | |
| Blood vessel invasion | | | >.999 | | | .096 | | | .150 |
| Present | 29 | 79 | | 56 | 52 | | 60 | 48 | |
| Absent | 16 | 41 | | 38 | 19 | | 39 | 18 | |
| Lymph node metastasis | | | .411 | | | .003 | | | .022 |
| Present | 29 | 67 | | 45 | 51 | | 50 | 46 | |
| Absent | 16 | 53 | | 49 | 20 | | 49 | 20 | |
| Liver metastasis | | | .044 | | | .101 | | | .052 |
| Present | 1 | 18 | | 7 | 12 | | 7 | 12 | |
| Absent | 44 | 102 | | 87 | 59 | | 92 | 54 | |
| Lung metastasis | | | .071 | | | .030 | | | .014 |
| Present | 1 | 16 | | 5 | 12 | | 5 | 12 | |
| Absent | 44 | 104 | | 89 | 59 | | 94 | 54 | |

* Data are given as number of cases or mean – SD. *P* values were calculated by using the Mann-Whitney *U* test for age and maximum tumor diameter, the Student *t* test for macroscopic type, and the $\chi^2$ test for all others.
† According to the World Health Organization classification: 1, polypoid; 2, ulcerating circumscribed; 3, ulcerating infiltrative; 4, diffusely infiltrative.
‡ According to the International Union Against Cancer TNM classification: T2, tumor invades the muscularis propria; T3, tumor invades through the muscularis propria into the subserosa or into nonperitonealized pericolic or perirectal tissues; T4, tumor directly invades other organs or structures and/or perforates the visceral peritoneum.
§ According to the World Health Organization classification: grade 1, well-differentiated adenocarcinoma; grade 2, moderately differentiated adenocarcinoma; grade 3, poorly differentiated adenocarcinoma, mucinous adenocarcinoma, and signet-ring cell carcinoma; grade 4, undifferentiated carcinoma.


DOI: 10.1309/AJCPK35VZJEWCUTL

were also positive for CXCL12. In addition, fibroblasts adjacent to cancer cells, as well as normal areas, were weakly positive, but their expression was significantly weaker than that of tumor cells. CXCL12 staining was localized diffusely or patchily, and CXCL12 was often expressed in tumor buds at the invasive front **Image 1B**.

The mean – SD proportion of CXCL12+ tumor cells was 60.8% – 27.3%. Of the 165 cases, 120 (72.7%) exhibited immunopositivity in 50% or more of the cancer cells.

Patients whose tumors had high CXCL12 expression had significantly shorter survival than patients whose tumors had low CXCL12 expression ($P = .014$ and $P = .005$, overall and recurrence-free survival rates, respectively; log-rank test) **Figure 1**. The correlations between the percentage of CXCL12 immunopositivity and clinicopathologic findings are shown in Table 1. The percentage of CXCL12 immunopositivity was correlated with the depth of tumor invasion, tumor budding grade determined by H&E staining, and liver metastasis.

The results of univariate analysis using the Cox proportional hazards model are shown in **Table 2**. CXCL12 expression was found to be a significant prognostic factor for overall and recurrence-free survival, together with depth of tumor invasion, tumor budding grade by H&E staining, and lymph node metastasis. In addition, blood vessel invasion was found to be a significant predictive factor for recurrence, whereas lymphatic vessel invasion tended to be predictive of recurrence. Multivariate analysis using the Cox proportional hazards model revealed that the percentage of CXCL12 immunopositivity and lymph node metastasis were independent prognostic factors for overall and recurrence-free survival **Table 3**.

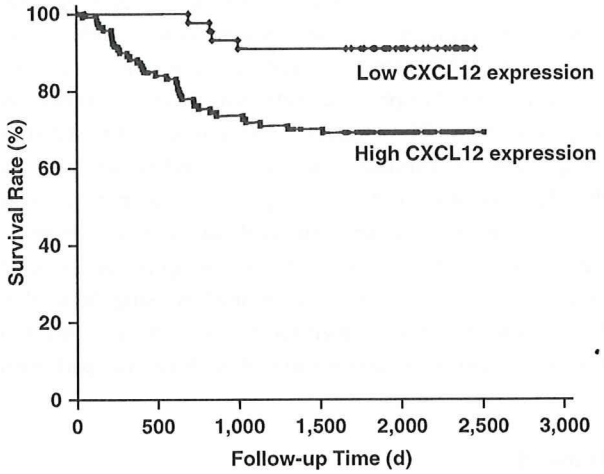


**Figure 1** Kaplan-Meier survival curves of patients with colorectal carcinoma subdivided according to the proportion of tumor cells expressing CXCL12 ($P = .014$; log-rank test).

### Grade of CXCL12 Immunopositivity in Foci of Tumor Budding

Of the 165 cases, 71 (43.0%) were defined as high grade, and the survival of the patients was significantly shorter than that of patients with low-grade tumors ($P = .003$ and $P < .001$, overall and recurrence-free survival rates, respectively; log-rank test) **Figure 2**. The number of CXCL12+ budding foci was correlated with the depth of tumor invasion ($P < .001$), tumor budding grade by H&E

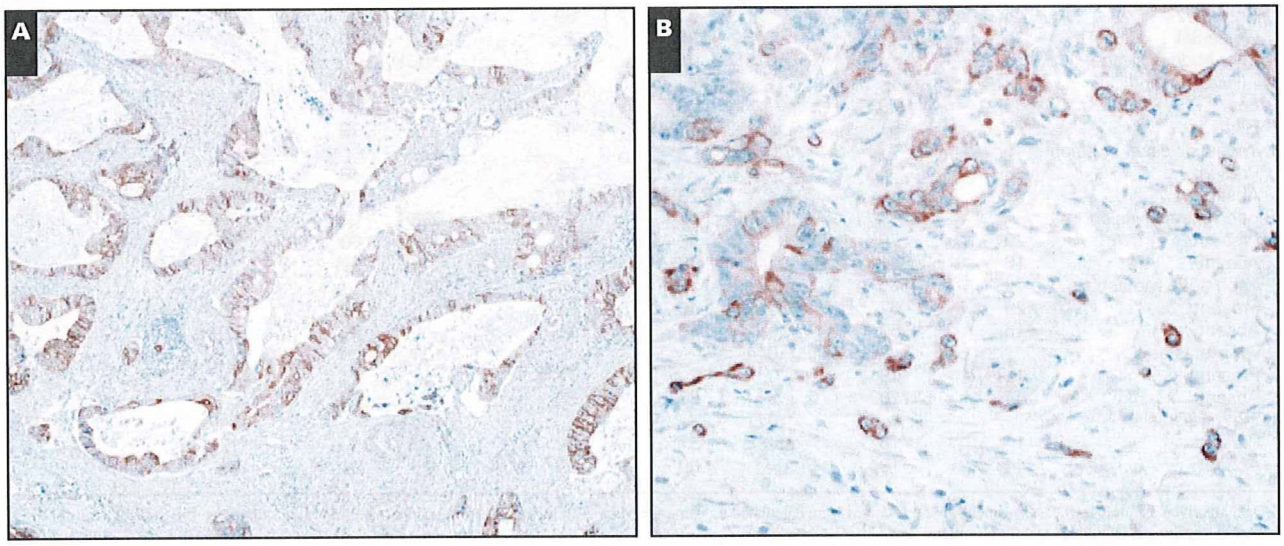


**Image 1** Immunohistochemical studies of CXCL12 in colorectal carcinoma. **A**, CXCL12 expression was observed in the cell membrane and cytoplasm of colorectal tumor cells. In this case, almost all tumor cells expressed CXCL12 (×45). **B**, CXCL12 expression was intense in tumor budding foci at the invasive front (×230).




DOI: 10.1309/AJCPK35VZJEWCUTL

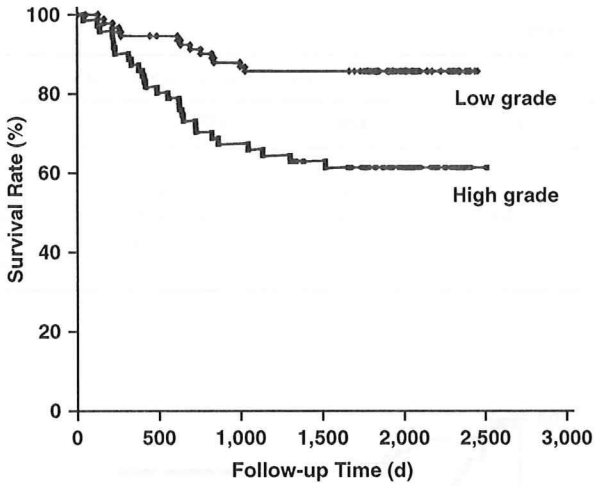


**Figure 2** Kaplan-Meier survival curves of patients with colorectal carcinoma subdivided according to the grade of CXCL12+ tumor budding ($P = .003$; log-rank test).

staining ($P < .001$), lymph node metastasis ($P = .003$), and lung metastasis ($P = .030$) (Table 1). Univariate analysis using the Cox proportional hazards model revealed that the grade of CXCL12-immunopositive tumor budding was a significant prognostic factor (Table 2). Multivariate analysis using the Cox proportional hazards model revealed that only lymph node metastasis was an independent prognostic factor for overall survival and that CXCL12+ tumor budding grade was not an independent factor for overall or recurrence-free survival **Table 4**.

### Combination of CXCL12 Expression and CXCL12+ Tumor Budding Grade

Patients with high CXCL12 expression and high-grade tumors had significantly shorter survival than patients with other combinations ($P < .001$ and $P < .001$, overall and recurrence-free survival rates, respectively; log-rank test) **Figure 3**. This combination was correlated with the depth of tumor invasion ($P < .001$), tumor budding grade by H&E

**Table 2**
**Univariate Cox Proportional Hazards Analysis for the Candidate Variables***

| | Overall Survival | | | Recurrence-Free Survival | | |
|---|---|---|---|---|---|---|
| **Prognostic Factor** | **HR** | **95% CI** | ***P*** | **HR** | **95% CI** | ***P*** |
| CXCL12 expression | 3.992 | 1.210-13.167 | .023 | 3.991 | 1.420-11.219 | .009 |
| CXCL12+ tumor budding grade | 3.036 | 1.420-6.493 | .004 | 3.140 | 1.619-6.091 | .001 |
| CXCL12 expression and CXCL12+ tumor budding grade | 3.540 | 1.655-7.574 | .001 | 3.659 | 1.886-7.098 | <.001 |
| Age | 1.013 | 0.538-1.906 | .969 | 0.949 | 0.464-1.941 | .885 |
| Sex | 1.139 | 0.609-2.133 | .684 | 1.855 | 0.826-4.168 | .134 |
| Tumor location | 1.118 | 0.573-2.430 | .653 | 1.139 | 0.609-2.133 | .684 |
| Tumor size | 1.119 | 0.546-2.293 | .760 | 0.889 | 0.478-1.654 | .711 |
| Macroscopic type | 0.977 | 0.278-3.429 | .970 | 1.218 | 0.382-3.885 | .740 |
| Tumor depth (T2, T3 vs T4) | 2.375 | 1.158-4.867 | .018 | 2.442 | 1.312-4.544 | .005 |
| Tumor differentiation (grade 1/2 vs grade 3/4) | 0.406 | 0.097-1.706 | .219 | 0.556 | 0.134-2.307 | .419 |
| Tumor budding grade (H&E staining) | 2.663 | 1.292-5.486 | .008 | 2.230 | 1.198-4.150 | .011 |
| Lymphatic vessel invasion | 2.032 | 0.709-5.824 | .187 | 2.789 | 0.992-7.839 | .052 |
| Blood vessel invasion | 2.081 | 0.893-4.853 | .090 | 2.516 | 1.159-5.463 | .020 |
| Lymph node metastasis | 5.454 | 1.902-15.639 | .002 | 3.326 | 1.532-7.222 | .002 |

HR, hazard ratio; CI, confidence interval.
* For descriptions of macroscopic type, tumor depth, and tumor differentiation, see the footnotes for Table 1.

**Table 3**
**Multivariate Cox Proportional Hazards Analysis for the Candidate Variables**

| | Overall Survival | | | Recurrence-Free Survival | | |
|---|---|---|---|---|---|---|
| **Prognostic Factor** | **HR** | **95% CI** | ***P*** | **HR** | **95% CI** | ***P*** |
| CXCL12 expression | 4.138 | 1.209-14.168 | .024 | 4.084 | 1.404-11.878 | .010 |
| Tumor depth* | 1.332 | 0.621-2.856 | .462 | 1.393 | 0.724-2.682 | .321 |
| Tumor budding grade (H&E staining) | 1.354 | 0.616-2.975 | .451 | 1.117 | 0.567-2.200 | .750 |
| Lymphatic vessel invasion | 1.047 | 0.323-3.398 | .939 | 1.576 | 0.516-4.810 | .424 |
| Blood vessel invasion | 1.179 | 0.461-3.019 | .731 | 1.535 | 0.657-3.582 | .322 |
| Lymph node metastasis | 5.063 | 1.654-15.493 | .005 | 2.781 | 1.200-6.444 | .017 |

HR, hazard ratio; CI, confidence interval.
* For description, see the footnotes for Table 1.


DOI: 10.1309/AJCPK35VZJEWCUTL

**Table 4**
**Multivariate Cox Proportional Hazards Analysis for the Candidate Variables**

| | Overall Survival | | | Recurrence-Free Survival | | |
|---|---|---|---|---|---|---|
| **Prognostic Factor** | **HR** | **95% CI** | ***P*** | **HR** | **95% CI** | ***P*** |
| CXCL12+ tumor budding grade | 1.859 | 0.782-4.417 | .160 | 2.099 | 0.998-4.415 | .051 |
| Tumor depth* | 1.422 | 0.624-3.242 | .402 | 1.406 | 0.702-2.814 | .336 |
| Lymphatic vessel invasion | 0.990 | 0.305-3.215 | .986 | 1.483 | 0.478-4.598 | .495 |
| Blood vessel invasion | 1.278 | 0.505-3.238 | .605 | 1.531 | 0.661-3.549 | .320 |
| Lymph node metastasis | 3.987 | 1.302-12.212 | .015 | 2.052 | 0.886-4.755 | .094 |

HR, hazard ratio; CI, confidence interval.
* For description, see the footnotes for Table 1.

staining ($P < .001$), lymph node metastasis ($P = .022$), and lung metastasis ($P = .014$). In addition, it showed a tendency to be correlated with liver metastasis ($P = .052$) (Table 1). Univariate analysis using the Cox proportional hazards model revealed that the combination of CXCL12 expression and CXCL12+ tumor budding grade was a significant prognostic factor (Table 2). Multivariate analysis using the Cox proportional hazards model revealed that the combination of CXCL12 expression and CXCL12+ tumor budding grade was an independent and significant prognostic factor for overall survival, together with lymph node metastasis, and also an independent prognostic factor for recurrence **Table 5**.

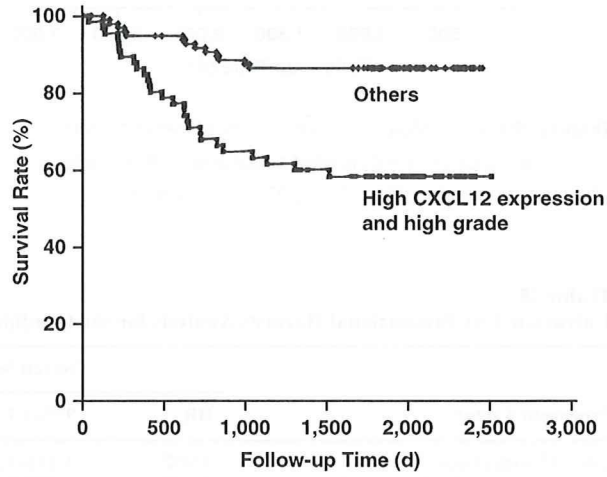


**Figure 3** Kaplan-Meier survival curves of patients with colorectal carcinoma subdivided according to the combination of the proportion of CXCL12 expression and the grade of CXCL12+ tumor budding ($P < .001$; log-rank test).

## Discussion

CXCL12 expression in colorectal cancer cells and at foci of tumor budding was found to be an independent predictive factor for cancer recurrence and poor survival. The present study indicated that CXCL12 expression in tumor cells was correlated with liver metastasis and was an independent prognostic factor together with lymph node metastasis. As it has been demonstrated that CXCL12 promotes tumor growth and malignancy,[21] colorectal cancers exhibiting high CXCL12 expression seem to show aggressive biologic behavior, with poor patient survival. To our knowledge, correlations between CXCL12 expression and long-term survival have been recognized in breast carcinoma,[21] ovarian

**Table 5**
**Multivariate Cox Proportional Hazards Analysis for the Candidate Variables**

| | Overall Survival | | | Recurrence-Free Survival | | |
|---|---|---|---|---|---|---|
| **Prognostic Factor** | **HR** | **95% CI** | ***P*** | **HR** | **95% CI** | ***P*** |
| CXCL12 expression and CXCL12+ tumor budding grade | 2.48 | 1.065-5.776 | .035 | 2.713 | 1.313-5.605 | .007 |
| Tumor depth* | 1.261 | 0.556-2.860 | .579 | 1.28 | 0.639-2.562 | .486 |
| Lymphatic vessel invasion | 1.061 | 0.324-3.478 | .922 | 1.571 | 0.504-4.892 | .436 |
| Blood vessel invasion | 1.26 | 0.496-3.203 | .627 | 1.51 | 0.650-3.504 | .338 |
| Lymph node metastasis | 3.932 | 1.296-11.929 | .016 | 2.056 | 0.895-4.721 | .089 |

HR, hazard ratio; CI, confidence interval.
* For description, see the footnotes for Table 1.




DOI: 10.1309/AJCPK35VZJEWCUTL

carcinoma,[19] glioma,[20] esophageal carcinoma,[17] and gastric carcinoma.[18] Immunohistochemical staining of frozen breast cancer tissues has demonstrated CXCL12 mostly in tumor cells and stromal cells, and the level of CXCL12 transcription in the tumor is correlated significantly with overall survival and incidence-free survival.[21] In addition, in this study, we noted that CXCL12 expression was stronger at the invasive front than in other areas of colorectal cancer, reflecting the fact that the invasive front shows the most active interaction between cancer and stroma. We therefore further focused on CXCL12 expression at sites of tumor budding.

Tumor budding has been reported to be related to metastatic activity[27,28] and prognostic outcome.[26,29] Although previous studies have addressed the prognostic impact of tumor budding, the assessment of tumor budding was done by counting tumor budding foci[24,25,30] or scoring the degree of tumor budding.[29,31,32] However, for objective quantification of tumor budding, it is necessary to apply immunostaining with the keratin cocktail AE1/AE3 and/or low-molecular-weight keratins (CAM5.2 [cytokeratins 8 and 18]). This approach highlights tumor buds extremely well and allows easy selection of counting areas and easy and rapid counting.[24,31] However, immunostaining with AE1/AE3 and/or CAM5.2 does not reflect the biologic activity of the tumor because all of the tumor cells are immunopositive.

In this study, we were able to count the numbers of tumor budding foci more easily than by H&E staining by using immunohistochemical analysis for CXCL12. CXCL12 immunostaining was used not only to highlight tumor cells but also to examine their potential aggressiveness by counting the number that were CXCL12+. CXCL12+ tumor budding grade was also correlated with the depth of tumor invasion, tumor budding grade determined by H&E staining, lymph node metastasis, and lung metastasis. CXCL12+ tumor budding grade was also demonstrated to be a prognostic indicator for overall survival and recurrence, although multivariate analysis showed that it was not an independent factor.

One reason why CXCL12+ tumor budding grade was not an independent factor may have been that the grade was judged in only 1 area where the budding foci were most intense and, therefore, probably did not reflect the properties of the whole tumor. Therefore, we combined the grading of CXCL12 immunopositivity for tumor buds with the proportion of tumor cells expressing CXCL12. We found that patients whose tumors showed high CXCL12 expression and high grade had the worst outcome. The combination of CXCL12 expression and CXCL12+ tumor budding grade was further correlated with the depth of tumor invasion, tumor budding grade determined by H&E staining, lymph node metastasis, and lung metastasis and tended to be correlated with liver metastasis. Moreover, this combination was an independent and significant prognostic factor for overall survival, together with lymph node metastasis, and also an independent prognostic factor for recurrence.

In our study, only a few grade 3 and 4 cases (5 of 165 cases) were included. Therefore, it seems possible that tumor differentiation did not affect the results of analyses. In general, the majority of colorectal carcinomas are diagnosed as grade 1 or 2, and the majority of grade 3 or 4 cases are included among cases that are more advanced than stage II or III.

In the present study, CXCL12 was expressed distinctly in colorectal cancer cells, normal epithelium of the colon (especially in the middle to upper third of each crypt in the mucosal layer), and blood and lymphatic endothelial cells and weakly in fibroblasts. Previous reports indicated that CXCL12 was constitutively expressed in various organs, including lymph nodes, lung, liver, thymus, and stromal cells such as fibroblasts, endothelial cells, and osteoblasts in bone marrow.[4,6,12]

Multiple biologic activities of CXCL12 have also been described.[7-10] For example, in vitro studies have shown that CXCL12 can modulate tumor cell proliferation and migration.[11,33,34] CXCL12 probably stimulates the formation of capillary-like structures by human vascular endothelial cells.[9,35,36] In addition, hypoxia-dependent up-regulation of the chemokine receptor CXCR4 practically promotes breast cancer invasion and organ-specific metastasis.[37,38] Colorectal carcinoma cells, especially those at the invasive front, are likely to be situated in a hypoxic milieu.[39,40] Therefore, this may lead to further tumor invasion through up-regulation of CXCL12/CXCR4.

CXCL12 expression in colorectal cancer cells and the grading of CXCL12 immunopositivity at foci of tumor budding are each significant prognostic factors. However, our present results suggest that, in colorectal carcinoma, CXCL12 expression used in combination with tumor budding grade is a more powerful prognostic indicator than either factor alone.

---

*From the [1]Pathology Division, National Cancer Center Research Institute, Tokyo, Japan; and [2]Surgery Division, National Cancer Center Hospital, Tokyo.*

*Supported in part by a Grant-in-Aid for the Third Term Comprehensive 10-Year Strategy for Cancer Control from the Ministry of Health, Labour and Welfare of Japan and grant 19790275 from the Ministry of Education, Culture, Sports, Science, and Technology of Japan.*

*Address reprint requests to Dr Akishima-Fukasawa: Pathology Division, National Cancer Center Research Institute, 5-1-1 Tsukiji, Chuo-ku, Tokyo 104-0045, Japan.*


DOI: 10.1309/AJCPK35VZJEWCUTL

## References


1. Ottaiano A, Franco R, Aiello Talamanca A, et al. Overexpression of both CXC chemokine receptor 4 and vascular endothelial growth factor proteins predicts early distant relapse in stage II-III colorectal cancer patients. *Clin Cancer Res.* 2006;12:2795-2803.
2. Liotta LA, Kohn EC. The microenvironment of the tumour-host interface. *Nature.* 2001;411:375-379.
3. Ibe S, Qin Z, Schuler T, et al. Tumor rejection by disturbing tumor stroma cell interactions. *J Exp Med.* 2001;194:1549-1559.
4. Shirozu M, Nakano T, Inazawa J, et al. Structure and chromosomal localization of the human stromal cell-derived factor 1 (*SDF1*) gene. *Genomics.* 1995;28:495-500.
5. Nagasawa T, Kikutani H, Kishimoto T. Molecular cloning and structure of a pre-B-cell growth-stimulating factor. *Proc Natl Acad Sci U S A.* 1994;91:2305-2309.
6. Tashiro K, Tada H, Heilker R, et al. Signal sequence trap: a cloning strategy for secreted proteins and type I membrane proteins. *Science.* 1993;261:600-603.
7. Fernandis AZ, Prasad A, Band H, et al. Regulation of CXCR4-mediated chemotaxis and chemoinvasion of breast cancer cells. *Oncogene.* 2004;23:157-167.
8. Nagasawa T, Tachibana K, Kishimoto T. A novel CXC chemokine PBSF/SDF-1 and its receptor CXCR4: their functions in development, hematopoiesis and HIV infection. *Semin Immunol.* 1998;10:179-185.
9. Salcedo R, Wasserman K, Young HA, et al. Vascular endothelial growth factor and basic fibroblast growth factor induce expression of CXCR4 on human endothelial cells: in vivo neovascularization induced by stromal-derived factor-1alpha. *Am J Pathol.* 1999;154:1125-1135.
10. Tachibana K, Hirota S, Iizasa H, et al. The chemokine receptor CXCR4 is essential for vascularization of the gastrointestinal tract. *Nature.* 1998;393:591-594.
11. Phillips RJ, Burdick MD, Lutz M, et al. The stromal derived factor-1/CXCL12-CXC chemokine receptor 4 biological axis in non-small cell lung cancer metastases. *Am J Respir Crit Care Med.* 2003;167:1676-1686.
12. Muller A, Homey B, Soto H, et al. Involvement of chemokine receptors in breast cancer metastasis. *Nature.* 2001;410:50-56.
13. Zeelenberg IS, Ruuls-Van Stalle L, Roos E. The chemokine receptor CXCR4 is required for outgrowth of colon carcinoma micrometastases. *Cancer Res.* 2003;63:3833-3839.
14. Schimanski CC, Schwald S, Simiantonaki N, et al. Effect of chemokine receptors CXCR4 and CCR7 on the metastatic behavior of human colorectal cancer. *Clin Cancer Res.* 2005;11:1743-1750.
15. Kaifi JT, Yekebas EF, Schurr P, et al. Tumor-cell homing to lymph nodes and bone marrow and CXCR4 expression in esophageal cancer. *J Natl Cancer Inst.* 2005;97:1840-1847.
16. Taichman RS, Cooper C, Keller ET, et al. Use of the stromal cell-derived factor-1/CXCR4 pathway in prostate cancer metastasis to bone. *Cancer Res.* 2002;62:1832-1837.
17. Sasaki K, Natsugoe S, Ishigami S, et al. Expression of CXCL12 and its receptor CXCR4 correlates with lymph node metastasis in submucosal esophageal cancer. *J Surg Oncol.* 2008;97:433-438.
18. Ishigami S, Natsugoe S, Okumura H, et al. Clinical implication of CXCL12 expression in gastric cancer. *Ann Surg Oncol.* 2007;14:3154-3158.
19. Jiang YP, Wu XH, Shi B, et al. Expression of chemokine CXCL12 and its receptor CXCR4 in human epithelial ovarian cancer: an independent prognostic factor for tumor progression. *Gynecol Oncol.* 2006;103:226-233.
20. Salmaggi A, Gelati M, Pollo B, et al. CXCL12 expression is predictive of a shorter time to tumor progression in low-grade glioma: a single-institution study in 50 patients. *J Neurooncol.* 2005;74:287-293.
21. Kang H, Watkins G, Parr C, et al. Stromal cell derived factor-1: its influence on invasiveness and migration of breast cancer cells in vitro, and its association with prognosis and survival in human breast cancer. *Breast Cancer Res.* 2005;7:R402-R410.
22. Sobin L, Wittekind C; for the International Union Against Cancer (UICC), eds. *TNM Classification of Malignant Tumours.* 6th ed. New York, NY: Wiley-Liss; 2002.
23. Hamilton SR, Aaltonen LA. *Pathology and Genetics of Tumours of the Digestive System.* Lyon, France: IARC Press; 2000. *World Health Organization Classification of Tumours.*
24. Prall F, Nizze H, Barten M. Tumour budding as prognostic factor in stage I/II colorectal carcinoma. *Histopathology.* 2005;47:17-24.
25. Ueno H, Price AB, Wilkinson KH, et al. A new prognostic staging system for rectal cancer. *Ann Surg.* 2004;240:832-839.
26. Ueno H, Murphy J, Jass JR, et al. Tumour "budding" as an index to estimate the potential of aggressiveness in rectal cancer. *Histopathology.* 2002;40:127-132.
27. Okuyama T, Oya M, Ishikawa H. Budding as a risk factor for lymph node metastasis in pT1 or pT2 well-differentiated colorectal adenocarcinoma. *Dis Colon Rectum.* 2002;45:628-634.
28. Goldstein NS, Hart J. Histologic features associated with lymph node metastasis in stage T1 and superficial T2 rectal adenocarcinomas in abdominoperineal resection specimens: identifying a subset of patients for whom treatment with adjuvant therapy or completion abdominoperineal resection should be considered after local excision. *Am J Clin Pathol.* 1999;111:51-58.
29. Hase K, Shatney C, Johnson D, et al. Prognostic value of tumor "budding" in patients with colorectal cancer. *Dis Colon Rectum.* 1993;36:627-635.
30. Ueno H, Mochizuki H, Hashiguchi Y, et al. Predictors of extrahepatic recurrence after resection of colorectal liver metastases. *Br J Surg.* 2004;91:327-333.
31. Kazama S, Watanabe T, Ajioka Y, et al. Tumour budding at the deepest invasive margin correlates with lymph node metastasis in submucosal colorectal cancer detected by anticytokeratin antibody CAM5.2. *Br J Cancer.* 2006;94:293-298.
32. Nakamura T, Mitomi H, Kikuchi S, et al. Evaluation of the usefulness of tumor budding on the prediction of metastasis to the lung and liver after curative excision of colorectal cancer. *Hepatogastroenterology.* 2005;52:1432-1435.
33. Brand S, Dambacher J, Beigel F, et al. CXCR4 and CXCL12 are inversely expressed in colorectal cancer cells and modulate cancer cell migration, invasion and MMP-9 activation. *Exp Cell Res.* 2005;310:117-130.
34. Scotton CJ, Wilson JL, Scott K, et al. Multiple actions of the chemokine CXCL12 on epithelial tumor cells in human ovarian cancer. *Cancer Res.* 2002;62:5930-5938.
35. Salcedo R, Oppenheim JJ. Role of chemokines in angiogenesis: CXCL12/SDF-1 and CXCR4 interaction, a key regulator of endothelial cell responses. *Microcirculation.* 2003;10:359-370.
36. Mirshahi F, Pourtau J, Li H, et al. SDF-1 activity on microvascular endothelial cells: consequences on angiogenesis in in vitro and in vivo models. *Thromb Res.* 2000;99:587-594.





DOI: 10.1309/AJCPK35VZJEWCUTL

37. Phillips RJ, Mestas J, Gharaee-Kermani M, et al. Epidermal growth factor and hypoxia-induced expression of CXC chemokine receptor 4 on non-small cell lung cancer cells is regulated by the phosphatidylinositol 3-kinase/PTEN/AKT/mammalian target of rapamycin signaling pathway and activation of hypoxia inducible factor-1alpha. *J Biol Chem.* 2005;280:22473-22481.
38. Matteucci E, Locati M, Desiderio MA. Hepatocyte growth factor enhances CXCR4 expression favoring breast cancer cell invasiveness. *Exp Cell Res.* 2005;310:176-185.
39. Sullivan R, Graham CH. Hypoxia-driven selection of the metastatic phenotype. *Cancer Metastasis Rev.* 2007;26:319-331.
40. Zhong H, De Marzo AM, Laughner E, et al. Overexpression of hypoxia-inducible factor 1alpha in common human cancers and their metastases. *Cancer Res.* 1999;59:5830-5835.


DOI: 10.1309/AJCPK35VZJEWCUTL

Clinical Translational Research

Oncology

Oncology 2009;77:53–62
DOI: 10.1159/000226112

Received: September 24, 2008
Accepted after revision: February 16, 2009
Published online: June 25, 2009

# Podoplanin Expression Identified in Stromal Fibroblasts as a Favorable Prognostic Marker in Patients with Colorectal Carcinoma

Takahiro Yamanashi[a, c] Yukihiro Nakanishi[a] Gen Fujii[a] Yuri Akishima-Fukasawa[a]
Yoshihiro Moriya[b] Yae Kanai[a] Masahiko Watanabe[c] Setsuo Hirohashi[a]

[a]Pathology and [b]Surgery Divisions, National Cancer Center Research Institute and Hospital, Tokyo, and
[c]Department of Surgery, Kitasato University School of Medicine, Kanagawa, Japan

**Key Words**
Podoplanin · Colorectal cancer · Prognosis · Immunohistochemistry · Clinicopathologic study

**Abstract**
***Objective:*** The microenvironment of cancer plays a critical role in its progression. However, the molecular features of cancer-associated fibroblasts (CAFs) are less well understood than those of cancer cells. We investigated the clinicopathological significance of podoplanin expression in stromal fibroblasts in patients with colorectal cancer (CRC). ***Methods:*** We selected podoplanin as an upregulated marker in CAF from a DNA microarray experiment. Consequently, podoplanin was identified as an upregulated gene. Immunohistochemical podoplanin expression was investigated at the National Cancer Center Hospital, Tokyo, Japan, in 120 patients with advanced CRC, and its clinicopathological significance was examined. The biological function of podoplanin expression was also assessed by a coculture invasion assay with CRC cell lines such as HCT116 and HCT15. ***Results:*** Podoplanin expression was exclusively confined to stromal fibroblasts and absent in tumor cells. Podoplanin is absent in normal stroma except for lymphatic vessels. Staining was considered positive when over 30% of the cancer stroma was stained. Positive podoplanin expression was significantly correlated with a more distal tumor localization ($p = 0.013$) and a shallower depth of tumor invasion ($p = 0.011$). Univariate analysis revealed that negative podoplanin expression in stromal fibroblasts was significantly associated with reduced disease-specific survival ($p = 0.0017$) and disease-free survival ($p < 0.0001$). Multivariate analysis revealed that negative podoplanin expression ($p = 0.016$) and lymph node metastasis ($p = 0.027$) were significantly associated with disease-free survival. CRC cell invasion was augmented by coculture with CAFs that were treated with siRNA for podoplanin. ***Conclusions:*** Our results suggest that a positive podoplanin expression in stromal fibroblasts could have a protective role against CRC cell invasion and is a significant indicator of a good prognosis in patients with advanced CRC, supported by biological analysis showing that podoplanin expression in CAFs is associated with decreased CRC cell invasion.



## Introduction

Previous reports have indicated that tumor progression is influenced and controlled by cellular interaction derived from a complex relationship between stromal, epithelial, and extracellular matrix components [1–5].

KARGER

Fax +41 61 306 12 34
E-Mail karger@karger.ch
www.karger.com


0030–2414/09/0771–0053$26.00/0

Accessible online at:
www.karger.com/ocl

Yukihiro Nakanishi, MD, PhD
Department of Pathology, National Cancer Center Research Institute
5-1-1 Tsukiji, Chuo-ku, Tokyo 104-0045 (Japan)
Tel. +81 3 3542 2511, ext. 4206, Fax +81 3 3248 2463
E-Mail yukihironakanishi@hotmail.com

Studies of breast, prostate, colon cancer and melanoma have identified a 'reactive stroma' that is characterized by a modified extracellular matrix composition, increased microvessel density, and the presence of inflammatory cells and fibroblasts with an 'activated' phenotype [6–11]. These modified fibroblasts, often termed myofibroblasts or cancer-associated fibroblasts (CAFs), are considered to play a central role in the complex process of tumor-stroma interaction and consequent tumorigenesis [1–5]. Numerous studies have provided evidence for a cancer-promoting role of activated CAFs [1–5], which supposedly initiate and promote tumor progression through specific communications with cancer cells. On the other hand, some CAFs could have a protective role against colorectal cancer (CRC) cell invasion. Nevertheless, the signals that could explain the transition of a normal fibroblast into a CAF are not fully understood, and therefore it has been unclear how the stromal reaction in cancer tissue supports and regulates tumor progression.

Podoplanin is a 38-kDa mucin-type transmembrane glycoprotein with extensive O-glycosylation and a high content of sialic acid, and has been implicated in tumor progression [12–16]. Podoplanin homologs include OTS-8, RT140, gp38, canine gp40, human gp36, and murine PA2.26 [17]. Since podoplanin is expressed on lymphatic, but not on blood vessel endothelium, it is also widely used as a specific marker for lymphatic endothelial cells and lymphangiogenesis [18, 19]. It has been reported that podoplanin-deficient mice die at birth due to respiratory failure, exhibiting a phenotype of dilated, malfunctioning lymphatic vessels and lymphedema [20]. Experiments addressing this issue have revealed that podoplanin colocalizes with ezrin, ERM (ezrin-radixin-moesin)-protein, at the cellular membrane, and that podoplanin promotes relocalization of ezrin to filopodia-like structures and induces cell migration in the absence of epithelial-mesenchymal transition [21]. Additionally, there is evidence to suggest that podoplanin promotes platelet aggregation, and that it may also be involved in cancer cell migration, invasion, metastasis, and malignant progression [22, 23]. The expression of podoplanin is upregulated in a number of different tumor types, including squamous cell carcinoma [13, 24], malignant mesothelioma [25, 26], Kaposi's sarcoma and angiosarcoma [19], hemangioblastoma [27], testicular seminoma [28], and brain tumors [12, 29, 30]. However, the physiological function of podoplanin is still unknown. Also, the functional contribution of podoplanin to tumor progression has remained elusive. Only a few previous studies have investigated podoplanin in fibroblasts, where PA2.26 antigen, a podoplanin homolog, is involved in reactive processes during skin remodeling [31].

In the present study, we selected podoplanin as a good upregulated marker molecule in CAF from a DNA microarray experiment (data not shown). Podoplanin expression in advanced colorectal carcinoma was investigated immunohistochemically and its clinicopathological significance was examined. Furthermore, its function in fibroblasts was assessed by using a coculture invasion assay with CRC cell lines.

## Patients and Methods

*Patients and Samples for Immunohistochemistry*

One hundred twenty formalin-fixed and paraffin-embedded blocks of CRC were drawn from the files of the National Cancer Center Hospital (NCCH), Tokyo, Japan. All cases were surgically resected between July 1, 1996, and January 1, 1998, and diagnosed as primary advanced CRC. The patients included 76 (63.3%) males and 44 (36.7%) females ranging in age from 31 to 86 years (median 60 years). The patients were restricted to consecutive cases diagnosed as stage II (n = 50, 41.7%) or stage III (n = 70, 58.3%) pathologically, in which all patients had undergone curative resection and none received pre- or postoperative adjuvant chemotherapy or radiation therapy. No patients were excluded from this study because of adjuvant therapy. Follow-up studies were complete in all patients, with a period ranging from 0.1 months to 6.6 years (median 5.2 years). Seven (14.0%) patients at stage II and 22 (31.4%) at stage III developed recurrences, and 3 (6.0%) patients at stage II and 16 (22.9%) at stage III died of CRC. Among the cases showing recurrences, liver metastasis was observed in 5 (10.0%) stage II cases and 12 (17.1%) stage III cases. Clinicopathological factors were all classified according to the TNM classification of the International Union against Cancer [32]. Histologic classification of tumors was made according to the World Health Organization International Histological Classification of Tumors [33]. Among the study cases, 41 (34.2%) were classified as well differentiated adenocarcinoma, 75 (62.5%) as moderately differentiated adenocarcinoma, 3 (2.5%) as poorly differentiated adenocarcinoma, and 1 (0.8%) as mucinous adenocarcinoma.

*Immunohistochemistry*

Four-micrometer-thick sections of tissue samples of the 120 CRCs were stained for the selected molecule, podoplanin, which was identified as being overexpressed in CAFs. Sections were deparaffinized in xylene and rehydrated in a graded ethanol series. Staining was done at room temperature as follows: all sections were quenched with 3% hydrogen peroxide solution in alcohol for 20 min to block endogenous peroxidase activity. After several washes in phosphate-buffered saline (PBS; Sigma, St. Louis, Mo., USA), the sections were heated in an autoclave to 121°C for 10 min in 0.01 M citrate buffer (pH 6.0) for antigen retrieval. Blocking was performed with 2% normal swine serum (NSS; Dako, Glostrup, Denmark) in PBS for 30 min, and then the sections were incubated with monoclonal antibody directed against human podoplanin (anti-D2–40; Dako) for 1 h at 1:50 dilution. After washing

in PBS, the sections were incubated with biotinylated antibody against mouse immunoglobulin G (Vector Laboratories, Burlingame, Calif., USA) for 30 min at 1:200 dilution, followed by streptavidin-conjugated horseradish peroxidase (Dako). Diaminobenzidine was used as a chromogen. Sections were counterstained with hematoxylin and coverslipped using Promounter (Meisei Electric Co., Bangkok, Thailand). For the negative control, 2% NSS was used instead of the primary antibody. Lymphatic vessels in normal stroma were used as a positive control for podoplanin immunopositivity.

*Evaluation of Podoplanin Expression in CRCs*

Immunostained sections of the 120 CRCs were evaluated using a light microscope by two observers (T.Y. and Y.A-F.) who were blinded to the patient characteristics. Podoplanin was evaluated according to the following criteria: staining was considered positive when staining equal to or stronger than that of lymphatic vessels was observed; staining was considered negative when it was absent or weaker than that of lymphatic vessels. Positive staining was divided into two groups: group A showing positive staining of 30% or more of the cancer stroma, and group B showing staining of less than 30% of the cancer stroma. Cases that were negative for podoplanin expression were classified into group B.

*Statistical Analysis for Immunohistochemistry*

Statistical tests were performed with StatView version 5.0 (SAS, Cary, N.C., USA). The relationships between immunohistochemical findings and clinicopathological factors were analyzed using Fisher's exact test, the $\chi^2$ test, Student's t test, or the Mann-Whitney U test. Deaths from causes other than CRC were treated as censored cases. Overall survival, recurrence-free survival, and liver metastasis-free survival were measured from the date of surgery to the end of follow-up, recurrence, liver metastasis and death, respectively. Survival curves were made using the Kaplan-Meier method and compared using the log rank test. Both univariate and multivariate survival analyses were performed using the Cox proportional hazards regression model.

*Cell Culture*

The human fibroblast cell line CCD-112CoN (CRL-1541) derived from normal colon tissue and the human CRC cell lines HT29, HCT116, and HCT15 were obtained from the American Type Culture Collection. CCD-112CoN cells were maintained in Eagle's Minimal Essential Medium (Gibco, Carlsbad, Calif., USA) supplemented with 10% fetal bovine serum (FBS; Gibco), 500 units/ml penicillin-streptomycin-fungizone (Gibco), 2 mmol/l L-glutamine (Gibco), and 1 mmol/l sodium pyruvate (Gibco). All CRC cell lines were maintained in RPMI-1640 medium (Sigma) supplemented with 10% FBS and antibiotics. All cell lines were cultured under conditions of 5% $CO_2$ in air at 37°C. CCD112CoN fibroblasts were used between the 25th and 30th passages for the experiments.

*Preparation of Cancer-Conditioned Medium*

Conditioned medium derived from cancer cell lines was used for induction of podoplanin in CAFs. After HT29 had been plated and allowed to attach to 75-$cm^2$ tissue culture dishes (Corning, Corning, N.Y., USA) for 24 h at subconfluency, the cells were rinsed twice with PBS and then incubated for another 72 h. The conditioned medium (CM) derived from HT29 (CM-HT29) was harvested, centrifuged at 200 *g* for 10 min to remove cell debris, and passed through a 0.2-μm filter (Millipore, Billerica, Mass., USA). Until use, the CM was stored at –20°C, which did not alter its biological activity (data not shown).

*Design of siRNA and Its Use for Transfection*

A siRNA duplex (sense, 5′-CAACAGUGUAACAGGCAUUdTdT-3′) specific for human podoplanin (GenBank accession No. NM_006474) was designed at Takara Bio Inc. (Shiga, Japan). Nonspecific control siRNA duplex with the same GC content as podoplanin siRNA (sense, 5′-AUACAGUGACAGCAACGUUdTdT-3′) was also purchased. Fibroblast cell line CCD-112CoN, in which podoplanin is not constitutively expressed in low-serum medium, was plated on 75-$cm^2$ tissue culture dishes in a subconfluent state. To create fibroblast cells expressing podoplanin, CCD-112CoN was allowed to adhere for 3 h in Eagle's Minimal Essential Medium with 10% FBS, washed twice with PBS and incubated in CM-HT29 with 10% FBS for 48 h. The cells were then plated on 6-well tissue culture plates at a density of $1.25 \times 10^5$ cells per well in CM-HT29 with 10% FBS. After overnight incubation, the cells were transfected with podoplanin siRNA or control siRNA at a final concentration of 100 nmol/l using LipofectAMINE 2000 (Invitrogen, Carlsbad, Calif., USA). For optimal transfection, a reduced serum medium (Opti-MEM; Gibco) was used to dilute the siRNA duplexes and LipofectAMINE 2000 according to the manufacturer's recommendations. Cells were used for Western blot analysis and Matrigel invasion assays after 72 h.

*Western Blot Analysis*

Cells were lysed in Tris-buffered saline-based lysis buffer (Tris-buffered saline, 1% Triton X-100, 0.5% sodium deoxycholate, 0.1% sodium lauryl sulfate, protease inhibitor), and protein concentration was determined using the Bio-Rad Protein Assay (Bio-Rad Laboratories, Hercules, Calif., USA). Equal amounts of proteins (10 μg) from the whole-cell lysates were separated by 10% SDS-PAGE and transferred to polyvinylidene difluoride membranes (Millipore). The membranes were blocked in TPBS (0.1% Tween 20 in PBS) solution with 5% nonfat dry milk for 1 h, then incubated with monoclonal antibody directed against human podoplanin (anti-D2–40; Dako) for 2 h at 1:100 dilution in blocking solution. Subsequently, the membranes were washed with TPBS, followed by incubation with horseradish-peroxidase-conjugated anti-mouse IgG antibody (GE Healthcare, Amersham, UK) for 1 h at 1:1,000 dilution. Immunoreactive proteins were detected using an enhanced chemiluminescence kit (GE Healthcare). β-Actin monoclonal antibody (Sigma) at 1:2,000 dilution was used as protein loading control.

*Matrigel Invasion Assay*

The transfected fibroblasts were cocultured with the invasive CRC cell lines (either HT116 or HT15) and analyzed using the BD BioCoat Matrigel Invasion Assay System (24-well BioCoat Matrigel invasion chambers; BD Bioscience, San Jose, Calif., USA) in accordance with the manufacturer's recommendations with minor modification. Briefly, after 24 h of transfection, the fibroblasts were plated on the upper chamber of the transwell insert (8-μm pores) in the presence or absence of CM-HT29 with 10% FBS at a density of $1 \times 10^4$ cells, and the lower wells contained the same medium. After overnight incubation, either HCT116 or

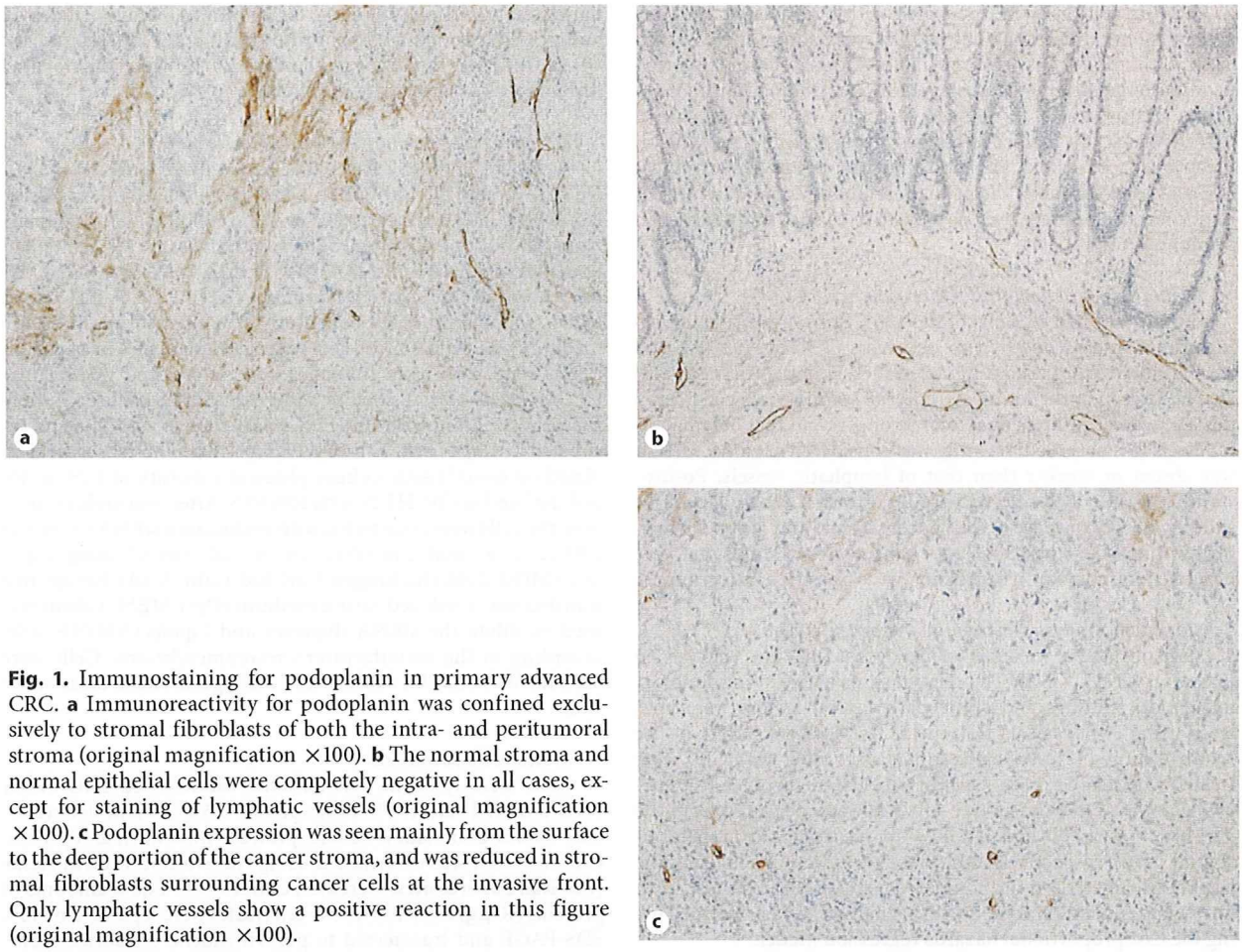

**Fig. 1.** Immunostaining for podoplanin in primary advanced CRC. **a** Immunoreactivity for podoplanin was confined exclusively to stromal fibroblasts of both the intra- and peritumoral stroma (original magnification ×100). **b** The normal stroma and normal epithelial cells were completely negative in all cases, except for staining of lymphatic vessels (original magnification ×100). **c** Podoplanin expression was seen mainly from the surface to the deep portion of the cancer stroma, and was reduced in stromal fibroblasts surrounding cancer cells at the invasive front. Only lymphatic vessels show a positive reaction in this figure (original magnification ×100).

HCT15 cells were seeded onto each of the upper chambers in CM-HT29 with 1% FBS at a density of 2 × $10^5$ cells, where the fibroblasts were in a confluent state. Carcinoma cells were allowed to migrate through both the transfected fibroblasts and the Matrigel matrix membrane for 24 h at 37°C. After incubation, the nonmigrated cells in the upper chamber were gently removed with a cotton swab, and the carcinoma cells that had invaded through the Matrigel-coated inserts were stained with Diff-Quik (Sysmex, Kobe, Japan). The number of carcinoma cells on the lower side in 5 randomly chosen areas per membrane was counted under a light microscope at ×100 magnification. Means were based on the numbers obtained from the 5 randomly chosen areas for each treatment condition. All assays were performed in triplicate, and the differences in the counts of cells that had invaded among the carcinoma cells that had been cocultured with fibroblasts transfected with either podoplanin siRNA or control siRNA were analyzed using Student's t test. Statistical tests were two-sided at a 5% level of significance.

## Results

*Podoplanin Expression in CRC*

Immunoreactivity for podoplanin was located in the cytoplasm and cell membrane of fibroblasts surrounding carcinoma cells. Immunoreactivity for podoplanin was confined exclusively to the stromal fibroblasts of both the intra- and the peritumoral stroma, and absent in stromal cells surrounding cancer cells budding from the tumor nests at the invasive front. Podoplanin expression was seen in stromal fibroblasts located mainly from the superficial to the deep area of the tumor, sparing the invasive front (fig. 1a–c), whereas normal stroma was completely negative in all cases except for lymphatic vessels (fig. 1). Podoplanin-positive staining was not observed in either normal epithelial cells or carcinoma cells. Fifty cases (41.7%) belonged to group A.

**Table 1.** Correlations between podoplanin expression and clinicopathological factors in patients with advanced CRC (stages II and III)

| Variables | Podoplanin | | p value |
|---|---|---|---|
| | group A (over 30) | group B (fewer than 30) | |
| Age, years | 60.0 ± 11.7 | 61.3 ± 10.7 | 0.5105[1] |
| Gender | | | |
| Male | 30 (25.0) | 46 (38.3) | |
| Female | 20 (16.7) | 24 (20.0) | 0.5219[2] |
| Tumor location | | | |
| Colon | 23 (19.2) | 48 (40.0) | |
| Rectum | 27 (22.5) | 22 (18.3) | 0.0131[2] |
| Maximum diameter of the tumor | | | 0.1565[3] |
| mm (median, range) | 42, 15–107 | 49, 15–110 | |
| Depth of invasion (pT)[4] | | | |
| T2 | 8 (6.7) | 2 (1.7) | |
| T3 | 42 (35.0) | 64 (53.3) | |
| T4 | 0 | 4 (3.3) | 0.0106[2] |
| Lymph node metastasis (pN) | | | |
| Absence | 25 (20.8) | 25 (20.8) | |
| Presence | 25 (20.8) | 45 (37.5) | 0.1176[2] |
| Histological grade[5] | | | |
| G1 | 19 (15.8) | 22 (18.3) | |
| G2 | 30 (25.0) | 45 (37.5) | |
| G3 | 1 (0.8) | 3 (2.5) | 0.634[2] |
| Lymphatic invasion | | | |
| Absence | 12 (10.0) | 13 (10.8) | |
| Presence | 38 (31.7) | 57 (47.5) | 0.4704[2] |
| Venous invasion | | | |
| Absence | 18 (15.0) | 17 (14.2) | |
| Presence | 32 (26.7) | 53 (44.2) | 0.164[2] |

Figures in parentheses are percentages.
[1] Student's t test.
[2] $\chi^2$ test or Fisher's exact test.
[3] Mann-Whitney U test.
[4] T2: tumor invades the muscularis propia; T3: tumor invades through the muscularis propia into the subserosa or peritoneal tissues; T4: tumor directly invades other organs or structures and/or perforates visceral peritoneum.
[5] G1: well-differentiated adenocarcinoma; G2: moderately differentiated adenocarcinoma; G3: poorly differentiated adenocarcinoma including signet ring cell adenocarcinoma and mucinous adenocarcinoma.

*Prognostic Value of Podoplanin Expression in Patients with CRC*

The correlations between podoplanin expression and clinicopathological factors are summarized in table 1. Group A was significantly correlated with a more distal tumor localization (p = 0.013) and a shallower depth of tumor invasion (p = 0.011) (table 1). There was no significant correlation between podoplanin expression, and age, gender, maximum tumor diameter, lymph node metastasis (pN), histological grade, lymphatic invasion, or venous invasion (table 1).

Patients in group A survived significantly longer than those who were negative, in terms of both disease-specific survival (DSS) and disease-free survival (DFS) (p = 0.0017 and p < 0.0001, respectively; fig. 2a, b). Patients in group A showed a significantly lower incidence of liver metastasis than patients in group B (p = 0.001; fig. 2c). For both DSS and DFS, univariate analysis using the Cox proportional hazards model revealed that podoplanin expression, depth of invasion (pT), and pN were significantly associated with prognosis (table 2), and that both podoplanin expression and pT were significantly associated with liver metastasis (table 2). Venous invasion factor tended to correlate with recurrence-free survival and liver metastasis-free survival (p = 0.086 and p = 0.051, respectively; table 2), but this tendency did not reach statistical significance. Multivariate analysis using the Cox proportional hazards model revealed that negative podoplanin expression and presence of pN were significantly associated with reduced DSS when adjusted for pT and venous invasion (p = 0.016 and p = 0.027, respectively; table 3). Multivariate analysis for both DFS and liver metastasis-free survival revealed that only podoplanin expression was associated with prognosis when adjusted for pT, pN, and venous invasion (p = 0.0023 and p = 0.020, respectively; table 3).

*Results of Invasion Assay*

To explore the biological role of podoplanin in fibroblasts, we used the RNA interference (RNAi) strategy to downregulate its expression. Increased podoplanin expression was observed in CAFs with CM-HT29, whereas it was not constitutively expressed in CCD112CoN cultured with low-serum medium. The podoplanin protein level in CAFs was substantially reduced within 72 h after transfection with 100 nmol/l podoplanin siRNA (fig. 3a). The result indicated that podoplanin siRNA effectively and specifically downregulated podoplanin protein expression in CAFs.

A tumor invasion assay was then performed using the Matrigel model to investigate whether reduced expression of podoplanin in CAFs increased the invasiveness of CRC cell lines in coculture. When CRC cell lines such as HCT116 and HCT15 were cocultured with CAFs transfected with control siRNA for podoplanin, a few invading cells were observed. However, when CRC cell lines were cocultured with CAFs transfected with siRNA1 for podo-